**CHARLES UNIVERSITY**
**Second Faculty of Medicine**

Summary of the Dissertation

# Selective regulation of presynaptic receptors by SGIP1

**Oleh Durydivka**

Prague, 2023

The dissertation was written during full-time doctoral study programme Biochemistry and Pathobiochemistry at the Institute of Molecular Genetics of the Czech Academy of Sciences.

Supervisor: doc. MUDr. Jaroslav Blahoš, Ph.D.
Institute of Molecular Genetics of the Czech Academy of Sciences, Vídeňská 1083, 142 20, Prague 4

Opponents:

The defence will take place before the Board for the Defence of the Subject Area Board Biochemistry and Pathobiochemistry on ..... in ..... ..... from ..... hours.

The Chairman of Subject Area Board and guarantor of the doctoral study programme Biochemistry and Pathobiochemistry:
prof. MUDr. Zdeněk Kleibl, Ph.D.
Institute of Medical Biochemistry and Laboratory Diagnostics, First Faculty of Medicine, Charles University and General University Hospital in Prague, Kateřinská 32, 128 00, Praha 2

The Dean of the Faculty: prof. MUDr. Marek Babjuk, CSc.

This work has been supported by grants GACR 19-24172S, GACR 21-02371S, and MEYS CZ.02.2.69/0.0/0.0/18_053/0016981.

The dissertation is available for inspection at the Department for Ph.D. Study of the Dean´s Office, Second Faculty of Medicine, Charles University, V Úvalu 84, 150 06 Praha 5 (phone 224 435 836).

# Table of contents

**Selective regulation of presynaptic receptors by SGIP1**


## Abstract

Cannabinoid receptor 1 (CB1R) is involved in a plethora of physiological processes, such as memory formation, motor coordination, anxiety, pain perception, and immune response. The properties of many minor cannabinoid receptor ligands remain unknown. The activity of CB1R is regulated by Src homology 3-domain growth factor receptor-bound 2-like endophilin interacting protein 1 (SGIP1). Several splice variants of SGIP1 have been described in the literature, but their specific functional roles are unknown. SGIP1 inhibits CB1R internalization and enhances β-arrestin and G protein-coupled receptor kinase 3 (GRK3) interactions with the receptor. In mice, deletion of *Sgip1* results in altered mood-related behavior, decreased anxiety-like behavior, and decreased acute nociception. In this work, we tested the effect of *Sgip1* deletion on chronic nociception. We further explored the pattern of alternative splicing of *Sgip1* in the brain. In addition, we tested the effect of the minor cannabinoid hexahydrocannabinol (HHC) on CB1R signaling. We found that *Sgip1* deletion results in an increase in chronic nociception in male but not in female mice. We detected 15 *Sgip1* splice variants in the mouse brain. The *Sgip1* exons that undergo alternative splicing encode portions of the MP domain and proline-rich region of the Sgip1 protein. We found that the pharmacological activity of (9R)-HHC epimer is higher than that of (9S)-HHC epimer, and the activity of (9R)-HHC epimer is similar to that of $\Delta^9$-tetrahydrocannabinol (THC). These results demonstrate that SGIP1 is an important player in pain sensitivity and other functions controlled by CB1R, that multiple *Sgip1* splice variants are expressed in the brain, and that cannabinoid HHC has similar properties to the common cannabinoid THC.



**Keywords**

alternative splicing, cannabinoid receptor 1, endocytosis, hexahydrocannabinol, nociception

# 1. Background

## Modulation of cannabinoid receptor 1 signaling by SGIP1

Cannabinoid receptor 1 (CB1R) is one of the most abundant G protein-coupled receptors (GPCR) in the brain [1]. CB1R is expressed at high levels in the neocortex, hippocampus, basal ganglia, cerebellum, and brainstem, as well as in the neurons of the dorsal root ganglia [2-6]. The activation of CB1R in the brain has been linked to a plethora of physiological functions, such as memory formation, motor coordination, appetite and metabolic control, thermoregulation, immune response, neurogenesis, anxiety, and analgesia, as well as to pathological conditions [1, 7, 8].

SGIP1 was identified as a CB1R-interacting partner using a yeast two-hybrid approach in our laboratory. SGIP1 associates with the C-terminal tail of CB1R [9, 10]. This association was verified by coimmunoprecipitation and bioluminescence resonance energy transfer (BRET) assay, and SGIP1 and CB1R colocalize in cultured neurons. When SGIP1 is co-expressed with CB1R in a heterologous system, such as HEK293 cells, this results in the inhibition of agonist-promoted endocytosis of CB1R. However, the interaction of GRK3 and β-arrestin with the activated CB1R is not inhibited; instead, it is enhanced and prolonged [9, 11]. At the same time, CB1R-dependent $G_{i/o}$ protein signaling was unaltered in the presence of SGIP1. On the other hand, the activity of the ERK1/2 pathway was inhibited in the presence of SGIP1 [9]. Thus, the effect of SGIP1 on the CB1R signaling is specific towards certain signaling pathways.

## *In vivo* implications of the CB1R-SGIP1 association

The effect of SGIP1 on CB1R has been evaluated *in vivo* by behavioral testing of *Sgip1* knock-out mice. These *Sgip1* knock-out mice had intact cognition and motor skills but exhibited altered mood-related behavior, decreased anxiety-like behavior, and decreased acute pain nociception [12]. The altered responses of the *Sgip1* knock-out mice to the cannabinoid tetrad tests demonstrate that *Sgip1* deletion affects the endocannabinoid system in the brain. These altered responses include anti-

nociception, catalepsy, and body temperature change. In addition, the *Sgip1* knock-out mice exhibited pronounced THC withdrawal signs manifested as intense jumping, which is characteristic of morphine withdrawal [12, 13].

**Expression pattern of SGIP1**

The isoforms of SGIP1, resulting from the alternative splicing of SGIP1 pre-mRNA, may differ in characteristics or functions. However, the available experimental works have focused on only one of the SGIP1 isoforms in regard to a particular function. For example, the SGIP1 806 isoform inhibits CB1R endocytosis [9], SGIP1 854 isoform controls the endocytosis and recycling of synaptotagmin 1 [14], SGIP1 826 isoform binds calnexin [15], and SGIP1 660 isoform increases CB1R expression in axons [10]. It is not known if these properties are specific to any isoform or if they are common for all SGIP1 isoforms. To date, only one study has attempted to compare two known SGIP1 isoforms [16], and no study has studied the splicing of SGIP1. The NCBI Gene database predicts that 20 *Sgip1* splice variants can be transcribed in mice. This prediction includes the four known variants but also provides 16 more variants. These variants, if experimentally detected, may provide new insights into SGIP1's functions, characteristics, and evolutional history.

**Novel cannabinoid ligands that mimic THC properties**

Hexahydrocannabinol (HHC) is a minor cannabinoid found in minute quantities in the cannabis plant, but it can be conveniently synthesized by acid treatment of CBD [17]. The production of semi-synthetic cannabinoid HHC is facilitated by the ease in the regulation of CBD production and use. Because HHC is not scheduled by the 1971 Convention on Psychotropic Substances, which controls tetrahydrocannabinol isomers only, HHC has emerged as a legal alternative to more commonly known THC; however, HHC might transition into a controlled substance category due to the insufficiency of comprehensive data regarding its activity, potency, toxicity, and overall safety [18-21].

## 2. Objectives

**Hypothesis 1.** SGIP1 is a CB1R-associated protein, and *Sgip1* deletion in mice reduces acute nociception and increases the potency of the analgesic effect of THC in the acute pain model. CB1R is involved in the processing of both acute and chronic pain. In chronic pain, pain processing circuits often become altered due to long-lasting activation, and the CB1R-SGIP1 relationship may be modified.

**Aim 1.** To determine the effect of *Sgip1* deletion on the sensitivity to mechanical stimulation in the mouse model of chronic inflammatory pain, induced by carrageenan injection, and the efficiency of THC-induced analgesic effect in this mouse model.

**Hypothesis 2.** SGIP1 has been reported as four splice isoforms in different studies; these isoforms are SGIP1 806, SGIP1 854 (termed SGIP1α), SGIP1 826, and SGIP1 660 (termed SGIP1β). The NCBI Gene database predicts that 20 *Sgip1* splice variants can be transcribed in mice. It is not known which splice variant is more abundant in the brain and if they have different properties.

**Aim 2.** To clone splice variants of *Sgip1* from the mouse brain, evaluate their relative abundance, compare their properties, and unify their nomenclature.

**Hypothesis 3.** The currently available drugs targeting CB1R are limited. The development of new drugs is hampered by the psychotropic effects of modulation of CB1R activity and other off-target effects. Minor constituents of the cannabis plant are being tested to explore their therapeutic potential. Among these constituents, HHC has gained much interest from researchers and public due to its THC-like effects and facile synthesis. Little information regarding HHC's effect on CB1R signaling is available; therefore, such HHC-induced signaling should be investigated and compared to commonly used cannabinoids.

**Aim 3.** To characterize the effect of the HHC epimers on the signaling pathways elicited by CB1R and compare their effects to those of THC and WIN.

# 3. Materials and methodology

## 3.1. The effect of Sgip1 on chronic pain in mice

Adult wild-type C57BL/6NCrl and *Sgip1* knock-out mice (characterized in [12]) were kept in a pathogen-free facility at 22 ± 2°C, 45% humidity, 12 h light/12 h dark cycle, and food and water *ad libitum*. Inflammatory pain in mice was induced by injecting 30 ul of 1% lambda carrageenan in normal saline into the left hind paw of the mice.

For the assessment of mechanical hyperalgesia, we applied a rigid plastic tip of an electronic von Frey instrument to the plantar surface of the hind paw until we observed a withdrawal response and recorded the pressure in grams. The von Frey tests were performed on day -1 (baseline), day 0 (2 h after the carrageenan injection), day 1 (1 h after the drug injection), and day 2. All the drugs were injected intraperitoneally at doses 10 mg/g, and the injection volume was 10 ul/g of mouse weight. The drugs were injected on day 1, and the behavioral testing was performed 1 h after the injections.

Withdrawal thresholds from five trials of the same mouse were averaged, and the resulting data are presented as means ± standard error of the mean (SEM). We applied the aligned rank transformation (ART) [22] and then conducted a repeated measures analysis of variance on linear models built from the transformed data. Significant interactions were further subjected to the Wilcoxon post hoc test with BH p adjustment method. Throughout the study, the following confidence thresholds were used: * $p < 0.05$, ** $p < 0.01$, *** $p < 0.001$.

## 3.2 Identification and characterization of Sgip1 splice variants in the brain

### 3.2.1. Cloning and expression of the *Sgip1* splice variants

To obtain RNA samples, we dissected the whole brain or prefrontal cortex (PFC), hippocampus (HC), and cerebellum (CB) of C57Bl/NCrl mice and used the TRIzol Plus RNA purification kit according to the manufacturer's instructions. Then, we used 5 μg of the obtained RNA in a reverse transcription reaction with 300 units (U)

of SuperScript III reverse transcriptase, 2.5 µg of an anchored oligo$(dT)_{20}$ primer, 0.5 mM of dATP, dGTP, dCTP, and dTTP each and 5 mM dithiothreitol (DTT) in 20 µL volume. Primer hybridization was at 65 °C for 5 min, followed by incubation at 4 °C for at least 1 min. First-strand complementary DNA (cDNA) synthesis was performed at 50 °C for 30 min, then at 55 °C for 30 min, followed by the enzyme inactivation at 70 °C for 15 min.

We amplified the *Sgip1* cDNA using Phusion High-Fidelity DNA polymerase with the primers annealing to the first and last exons of the *Sgip1* gene. The polymerase chain reaction (PCR) contained 0.2 U of the polymerase, 0.2 mM of dATP, dGTP, dCTP, and dTTP each, and 0.2 mM of each primer in 10 µL volume. For amplification, initial denaturation was at 98 °C, 30 s, followed by 30 cycles of denaturation at 98 °C, 30 s; annealing at 57.5 °C, 30 s and extension at 72 °C, 60 s each; the reaction ended with a final extension at 72 °C, 7 min.

Next, we purified the PCR products from 1.5% agarose gel using the QIAquick gel extraction kit. To prepare the PCR products for TA cloning, we added single A-overhangs to the products using 10 U of GoTaq G2 DNA polymerase, 2 mM dATP in 10 µL volume and incubated the reaction at 72 °C for 7 min. Then, we ligated the A-tailed products with pGEM-T Easy vector using T4 DNA ligase (3 U) in 10 µL volume. Last, we transformed chemically competent *E.coli* DH5α cells with the ligation reaction and spread the cells on Luria-Bertani (LB)-agar plates with 0.5 mM IPTG and 80 µg/mL X-Gal for blue-white colony screen.

For screening, we purified plasmid DNA from single white colonies propagated in LB medium containing 100 µg/mL ampicillin using the QIAprep Miniprep kit and digested the plasmid DNA with restriction enzymes EcoRI or EcoRI and XagI. Finally, the selected plasmids were sequenced by the dideoxy chain termination method.

To express Sgip1 splice isoforms in human embryonic kidney 293 (HEK293) cells, we transferred the coding sequence of the *Sgip1* splice variants from pGEM-T Easy vectors into pRK5 and pRK5-EYFP vectors. First, we released the insert from the

pGEM-T Easy vector by digestion with BamHI and SalI and purified it from 1.0% agarose gel using QIAquick gel extraction kit. Next, we ligated the inserts with the linearized pRK5 or pRK5-EYFP vectors using 0.5 U of T4 DNA ligase in 10 µL volume. The pRK5 vector expresses untagged Sgip1 splice isoforms, and pRK5-EYFP vector expresses the splice variants N-terminally tagged with EYFP with a Trp-Ile-Arg linker.

### 3.2.2. Microscopy and image processing

For microscopy, Human Embryonic Kidney 293 (HEK293) cells were cultured in DMEM – high glucose supplemented with 10% fetal bovine serum at 37 °C and 5% $CO_2$ in air and humidity of 95%. HEK293 cells grown on 18-mm glass coverslips were transfected with plasmid DNA encoding *Sgip1* splice variants using the calcium phosphate method. The plasmid DNA (1.2 µg) was mixed with 6.2 µL of 2 M $CaCl_2$ in a total volume of 50 µL, followed by the addition of the equal volume of 2x HBS (42 mM HEPES, 1.4 mM $Na_2HPO_4$, 274 mM NaCl, 10 mM KCl, 15 mM D-glucose, pH 7.05) and vigorous mixing. After 5 min of incubation, the transfection solution was added to the cells. The cells 24 h post-transfection were fixed in 4% paraformaldehyde in PBS for 15 min, then washed four times with PBS, rinsed with distilled water, dried and mounted in Fluoroshield mounting medium with DAPI. Microscopy was performed on Leica TCS SP8 confocal microscope using HC PL APO 63x/1.40 OIL objective and 2x digital zoom, resulting in a pixel size of 71 nm. The EYFP was excited with a 488 nm solid-state laser, and the EYFP emission was detected in a range of 498–542 nm using HyD detector at 50% gain. The images in a Z-plane were taken with a step of 0.299 µm. The microscopic images were processed in Fiji distribution of ImageJ 1.53c [23]. Z-stacks were projected using maximum intensity projection. Image adjustments, including brightness and contrast change, were applied to the whole area of the image.

### 3.2.8. Protein sample preparation

HEK293 cells were transfected with plasmid DNA encoding *Sgip1* splice variants using 90 μg of polyethylenimine and 30 μg of the DNA per $3 \times 10^6$ cells grown in a 10-cm plate and harvested 48 h after transfection. The samples from the prefrontal cortex, hippocampus, and cerebellum or the transfected HEK293 cells were homogenized in radioimmunoprecipitation assay (RIPA) buffer (50 mM Tris-HCl, 150 mM NaCl, 1% Triton X-100, 0.5% sodium deoxycholate, 0.1% sodium dodecyl sulfate (SDS), pH 8.0) supplemented with protease inhibitor cocktail and incubated with equal volumes of treatment buffer (125 mM Tris-HCl, 4% SDS, 20% glycerol, 0.02% bromophenol blue, 400 mM DTT, pH 6.8) for 5 min at 80 °C.

### 3.2.4. Immunoblot analysis

The protein samples were separated in SDS-polyacrylamide gel (SDS-PAGE) and transferred onto a nitrocellulose membrane using the Trans-Blot Turbo Transfer System. The membranes were blocked in 5% powdered milk in PBST (137 mM NaCl, 2.7 mM KCl, 8 mM $Na_2HPO_4$, 1.8 mM $KH_2PO_4$, 0.1% Tween 20) overnight at 4 °C. Then, the membranes were incubated with one of the primary antibodies as indicated. The guinea pig anti-Sgip1 antibody was diluted 1:500 to a final concentration of 0.0008 mg/mL in 2% milk in PBST and incubated for 3 h at 4 °C. The supernatant of the mouse anti-Sgip1 antibody-producing hybridoma was incubated with the membranes for 3 h at 4 °C. The anti-β-tubulin antibody was diluted 1:200 in 1% milk in PBST and incubated overnight at 4 °C. The anti-ubiquitin antibody was diluted 1:1000 in 2% milk in PBST and incubated for 3 h at 4 °C. After washing in PBST three times 15 min each, the membranes were incubated with the secondary antibody. The HRP-conjugated goat anti-guinea pig antibody diluted 1:5000 in 0.5% milk in PBST. The HRP-conjugated goat anti-mouse antibody and the HRP-conjugated goat anti-rabbit antibody were diluted 1:10 000 in 1% milk in PBST and incubated for 1 h at room temperature. The blots were

visualized using SuperSignal West Pico or Femto chemiluminescent substrates and detected on the Alliance Q9 Atom system.

### 3.3. Pharmacological evaluation of hexahydrocannabinol epimers

HEK293 cells were plated in the 96-well plates at 50 000 cells per well and transfected with 150 ng of plasmid DNA per well using Lipofectamine 2000 according to the manufacturer's instructions.

Bioluminescence resonance energy transfer (BRET) assay was used to measure CB1R-induced G protein dissociation and beta-arrestin interaction with CB1R, as described previously [9, 11]. To measure G protein dissociation, we transfected the cells with $G\alpha_{i1}$-Rluc8 or $G\alpha_{oA}$-Rluc8, $G\beta_2$-Flag, $G\gamma_2$-EYFP, and SNAP-CB1R plasmids in a mass ratio of 1:1:1:2. To measure β-arrestin 2 interaction with CB1R, we transfected the cells with β -arrestin2-Rluc and CB1R-YFP plasmids in a mass ratio of 1:2. To study GRK3-CB1R interaction, the cells were transiently transfected with GRK3-Rluc8 and CB1R-YFP plasmids (1:2 ratio). Before the measurements, the transfected cells were washed with PBS and incubated in Tyrode's solution at 37 °C for at least 30 min. Next, we added coelenterazine h at a final concentration of 5 μM to the cells, followed by the addition of increasing concentrations of compounds (9S)-HHC, (9R)-HHC, THC, WIN, or their vehicles. BRET donor and acceptor emission was measured 12 minutes after the addition of the compounds using Mithras LB940 plate reader.

The BRET ratio was obtained by dividing the acceptor emission (540 ± 20 nm) by the donor emission (480 ± 10 nm). After subtracting the BRET ratio of the vehicle addition from the BRET ratio of the compounds, we obtained deltaBRET (ΔBRET). Data analysis was performed using GraphPad Prism 9.3.1 for Windows. The dose-response curves were fitted using the non-linear regression function.

# 4. Results

## 4.1. The effect of Sgip1 on chronic pain processing

To test the effect of *Sgip1* deletion on chronic nociception, we induced chronic inflammatory pain in wild-type and *Sgip1* knock-out mice and evaluated the mechanical sensitivity of these mice. Inflammation was induced by carrageenan injection in the hind paw, which caused edema, hyperalgesia, and mechanical allodynia. We measured the sensitivity to mechanical stimulation by applying the rigid tip of the electronic von Frey apparatus to the hind paw of the mice. To evaluate the changes in mechanical nociception in the mice after the carrageenan injection, we applied the following scheme. On day -1, we measured the baseline responses in all the mice. On day 0, we injected carrageenan or vehicle (saline) in one hind paw and measured the mechanical sensitivity 2 h after the injection. We then repeated the measurements until 3 days after the injection to monitor the course of inflammation.

Carrageenan injection caused a decrease in the withdrawal threshold of the paw, reflecting increased sensitivity to the mechanical stimulation 2 h after the injection. This decrease in paw withdrawal threshold persisted for two days after the injection, which is characteristic of carrageenan-induced inflammation. Vehicle injection did not affect the mechanical sensitivity. In male mice, the paw withdrawal threshold of *Sgip1* knock-out mice was significantly lower ($p = 0.0317$ on Day 1 after the carrageenan injection) than that of wild-type mice, and this difference persisted throughout the course of the inflammation (Figure 1A).

Because vehicle injection did not affect the paw withdrawal threshold of the male mice, we injected the female mice with carrageenan only. We found that in the female mice, the paw withdrawal threshold of *Sgip1* knock-out mice was not different from that of wild-type mice (Figure 1B).

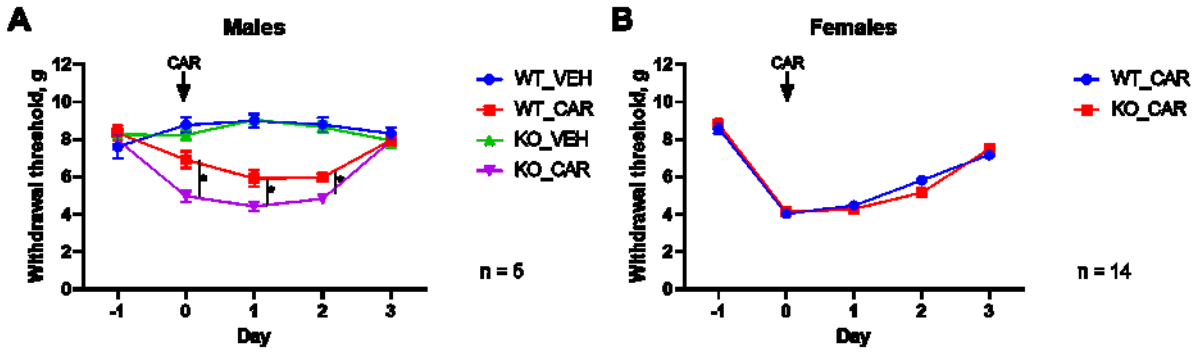


**Figure 1.** The effect of *Sgip1* deletion on mechanical sensitivity of male (A) and female (B) mice. Baseline sensitivity of the left hindpaw of wild-type (WT) and *Sgip1* knock-out (KO) mice was determined on day -1, and carrageenan (CAR) was injected into the left hindpaw on day 0. Each point is the mean ± SEM of 5 (male) or 14 (female) mice.

### 4.1.2. The effects of cannabinoids on chronic pain sensitivity

WIN 55,212-2 (WIN) injection in males increased the threshold of *Sgip1* knock-out mice by 77% and that of wild-type mice by 91%. The threshold of WIN-treated *Sgip1* knock-out males was significantly lower ($p = 0.0232$) than that of wild-type males (Figure 2A). WIN injection in females increased the threshold of *Sgip1* knock-out mice by 75% and that of wild-type mice by 96%. However, the threshold of WIN-treated *Sgip1* knock-out females was similar to that of wild-type females (Figure 2B).

After $\Delta^9$-tetrahydrocannabinol (THC) injections, the mechanical thresholds of male mice followed a pattern similar to the WIN injections. THC in males led to a 63% increase in the threshold of *Sgip1* knock-out mice and a 55% increase in wild-type mice. The threshold of THC-treated *Sgip1* knock-out males was significantly higher ($p = 0.00376$) than that of wild-type males (Figure 3A). THC treatment of females led to a 60% increase in the threshold of *Sgip1* knock-out mice and only a 28% increase in wild-type mice. As a result, the threshold of THC-treated *Sgip1* knock-out females was significantly higher ($p = 0.00935$) than that of wild-type females (Figure 3B).

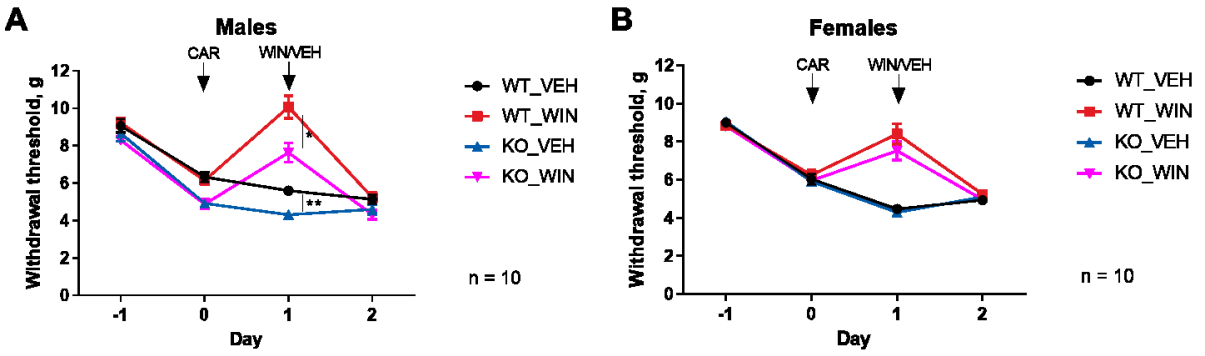


**Figure 2.** The effect of WIN 55,212-2 (WIN) and deletion of *Sgip1* on mechanical sensitivity of male (A) and female (B) mice. Baseline sensitivity of the left hindpaw of wild-type (WT) and *Sgip1* knock-out (KO) mice was determined on day -1, carrageenan (CAR) was injected on day 0, and 10 mg/kg WIN or vehicle (VEH) was injected on day 1. Each point is the mean ± SEM of 10 mice.

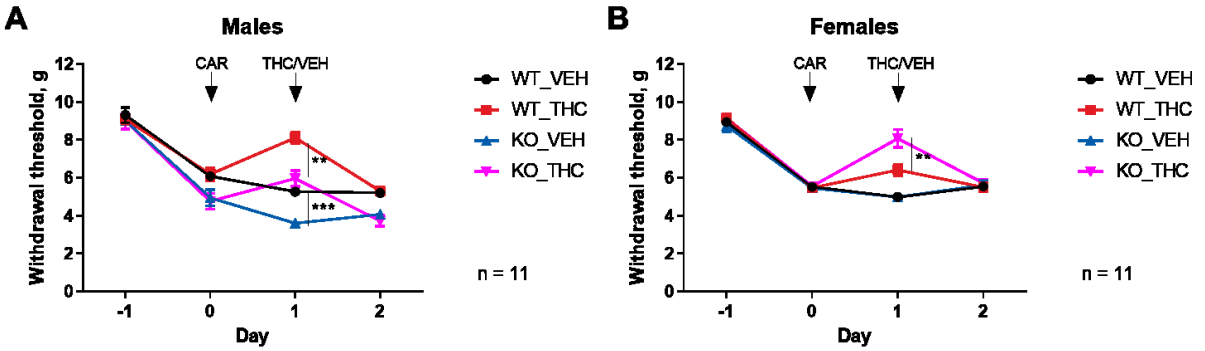


**Figure 3.** The effect of $\Delta^9$-tetrahydrocannabinol (THC) and deletion of *Sgip1* on mechanical sensitivity of male (A) and female (B) mice. Baseline sensitivity of the left hindpaw of wild-type (WT) and *Sgip1* knock-out (KO) mice was determined on day -1, carrageenan (CAR) was injected on day 0, and 10 mg/kg THC or vehicle (VEH) was injected on day 1. Each point is the mean ± SEM of 11 mice.

## 4.2. Identification and characterization of *Sgip1* splice variants in the brain

### 4.2.1. Expression patterns of *Sgip1* in the brain

We analyzed samples prepared from the mouse prefrontal cortex (PFC), hippocampus (HC), and cerebellum (CB) by immunoblotting that employs the anti-Sgip1 antibody. The anti-Sgip1 antibody recognized two immunoreactive bands in the PFC and HC samples and one band in the CB sample (Figure 4A). The upper

immunoreactive band was intensively stained and corresponded to a molecular weight of approximately 130 kDa. The bottom band was weakly stained and corresponded to 110 kDa. The staining intensity of the bottom band varied between the samples and was undetectable in the CB sample.

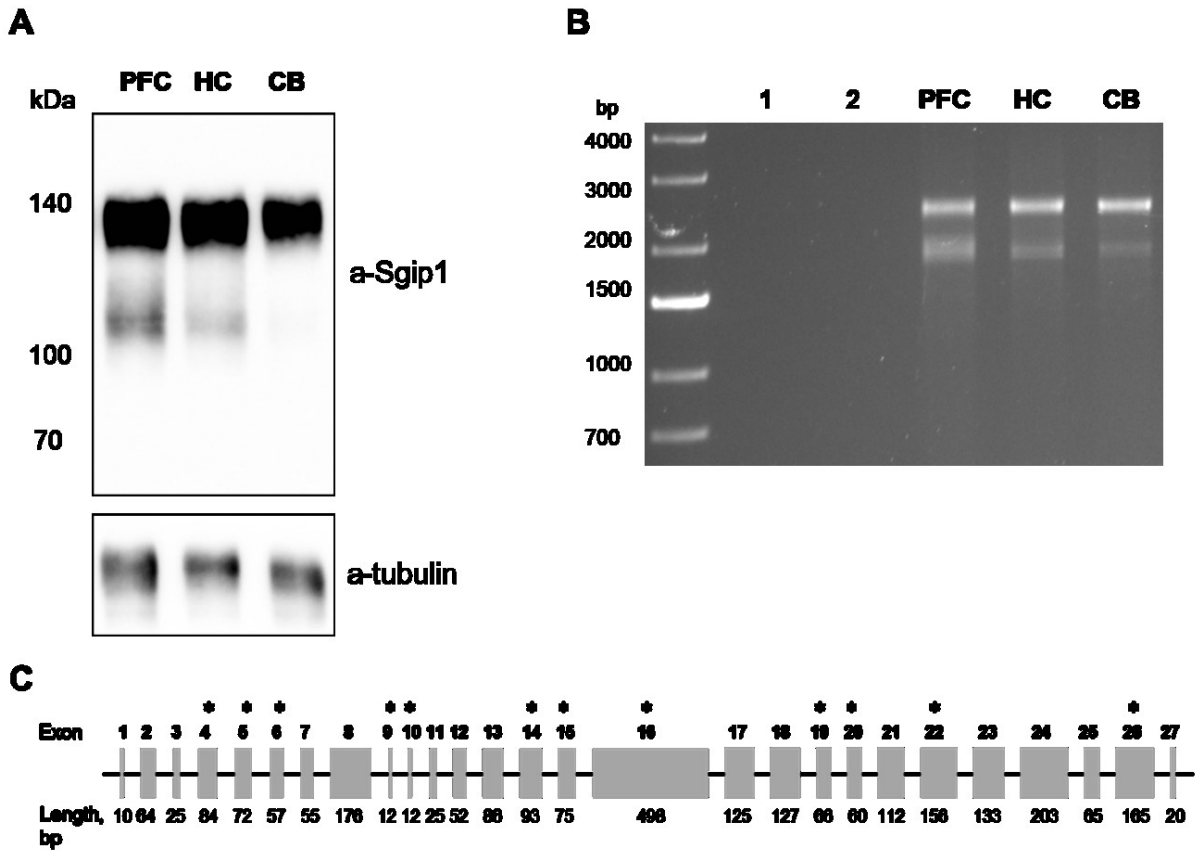


**Figure 4.** Expression patterns of *Sgip1* in the mouse brain. (A) The samples from the mouse prefrontal cortex (PFC), hippocampus (HC), and cerebellum (CB) were resolved in SDS-PAGE and probed with the anti-Sgip1 antibody. (B) The full-length *Sgip1* sequence was amplified in the RT-PCR using RNA obtained from the PFC, HC, and CB and resolved in an agarose gel. 1 - no PCR template control, 2 - no RT control. (C) The mouse *Sgip1* gene contains 27 exons, several of which allow in-frame deletion; these exons are marked with an asterisk (*).

Next, we investigated the pattern of the *Sgip1* gene transcripts. For this purpose, we obtained RNA samples from the same brain regions (PFC, HC, and CB) and synthesized cDNA. We then amplified the full-length *Sgip1* sequence by employing

primers annealing to the first and last exons of the *Sgip1* gene. Amplification of *Sgip1* cDNA resulted in products concentrated in two bands in the agarose gel (Figure 4B).

Based on the immunoblot and amplification patterns of *Sgip1*, it is possible that at least two *Sgip1* splice variants are present in the mouse brain: the longer, more abundant variant and the shorter, less abundant one. These two splice variants may constitute the two bands that we detected in our samples. According to the NCBI Gene and Ensembl databases, the mouse *Sgip1* gene contains 27 exons, 12 of which do not create a frameshift mutation when omitted from the transcript (Figure 4C). The combinations of these 12 exons may potentially lead to the production of numerous isoforms of Sgip1.

### 4.2.2. Cloning and identification of *Sgip1* splice variants

To clone the *Sgip1* transcripts, we first amplified the full-length *Sgip1* coding sequence from the RNA isolated from the mouse brain (Figure 5A-B). Next, we purified the RT-PCR products from the two bands in the agarose gel and ligated the purified products with pGEM-T Easy vector. As a result, we created a library of *Sgip1* transcripts (Figure 5C). After the transformation of the *E.coli* cells and screening by restriction analysis, we obtained 15 unique non-redundant clones that can be discriminated by enzymatic digestion by EcoRI and XagI enzymes (Figure 5D). These 15 unique clones were further sequenced. In total, we analyzed 63 clones, and the numbers of clones containing each splice variant are provided in Table 10. The longest *Sgip1* transcript contained 27 exons (876 aa in length), and the shortest transcript contained only 20 exons (527 aa). Most *Sgip1* transcripts contained variations in exon composition within the N-terminal (exons 4-5) and central (exons 16, 20) regions (Figure 6). Some *Sgip1* splice variants resulted from alternative splicing by skipping exons 9-10, 15-19, or 19, and only one splice variant retained exon 19 (Figure 10). Due to the large number of the detected *Sgip1* splice variants, we indicate each *Sgip1* transcript with its length.

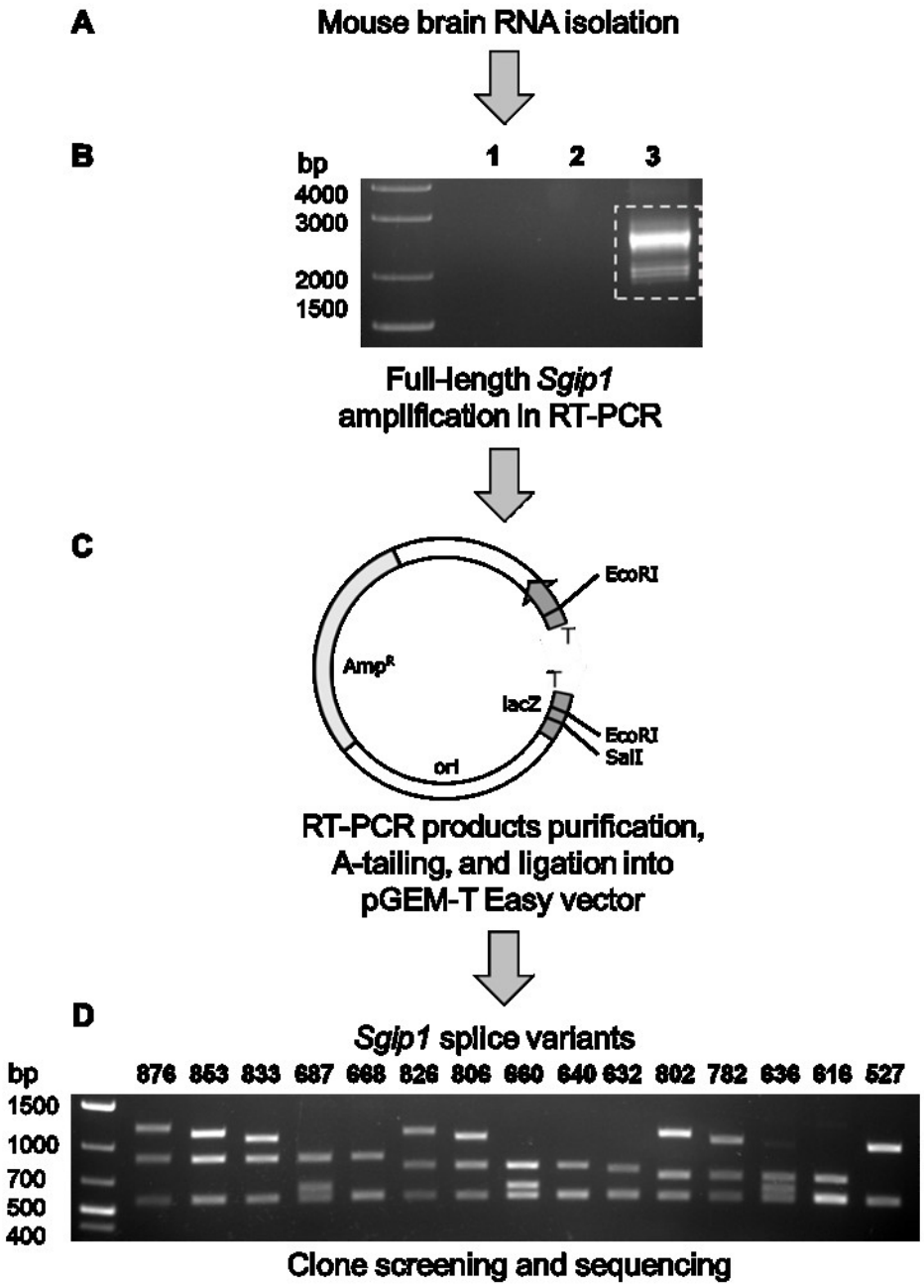


**Figure 5.** Cloning and identification of *Sgip1* spice variants. (A, B) The RNA from the mouse brain was used in RT-PCR employing an anchored oligo$(dT)_{20}$ primer and primers binding to the first and the last exon of the *Sgip1* gene. 1 - no PCR template control, 2 - no RT control, 3 - RT-PCR products. (C) The purified PCR products (dashed rectangle in Figure 9b) were ligated with pGEM-T Easy vector. (D) The colonies were screened by enzymatic digestion with EcoRI and XagI, and unique non-redundant clones were sequenced. Enzymatic digestion revealed patterns of bands unique for each splice variant. *Sgip1* splice variants are marked with their amino acid length (527-876).

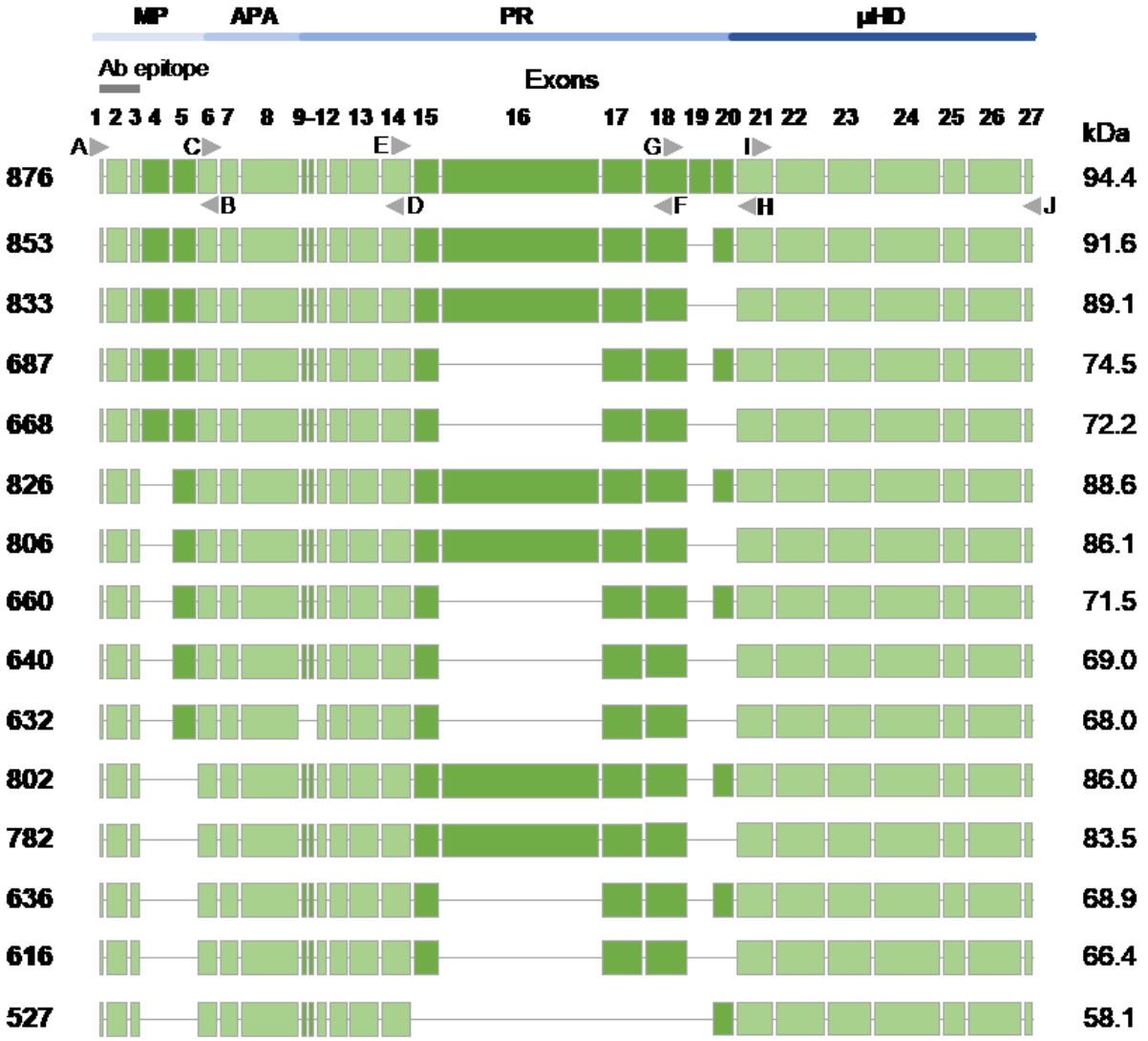


**Figure 6.** Schematic representation of the exon composition of the detected *Sgip1* splice variants. We detected 15 *Sgip1* splice variants, which are marked with their amino acid length (527-876). The variations in exon composition occur in the regions that correspond to two regions of Sgip1 protein: the MP domain and the proline-rich region. The domain structure of Sgip1 is represented by: MP - membrane phospholipid-binding domain, APA - AP2 activator domain, PR - proline-rich region, µHD - µ homology domain. The antibody (Ab) epitope indicates the recognition site of the anti-Sgip1 antibody that we used in the study. The primers used in the PCR within the study are marked with arrowheads and letters A-J. The estimated molecular weights of the proteins coded by the splice variants are provided in kDa.

### 4.2.3. Characterization of the expression of the *Sgip1* splice variants

We found that most *Sgip1* transcripts are alternatively spliced within the N-terminal (exons 4, 5) and central (exons 16, 20) regions of Sgip1. The variations in these regions may substantially affect the protein's properties. To test this possibility, we chose a subset of *Sgip1* splice variants that have various combinations of exons 4, 5, 16, and 20, namely *Sgip1* 853, *Sgip1* 826, *Sgip1* 806, *Sgip1* 802, *Sgip1* 660, and *Sgip1* 640 (Figure 7A), and tested the expression of these splice variants by fluorescent microscopy.

Next, we tested if the Sgip1 isoforms are properly localized in the cells. For this purpose, we transfected the cells with the EYFP-tagged *Sgip1* splice variants to assess their intracellular distribution by microscopy. We found that the splice variants were represented by a major pool of the protein located in the cytoplasm (Figure 7B), and a fraction of the proteins formed puncta at the plasma membrane (Figure 7B, insets). Except for the Sgip1 853 splice isoform, there were no apparent differences in the localization patterns between the Sgip1 isoforms, and this pattern was in line with the previous reports regarding the intracellular distribution of Sgip1 [24, 25]. However, in approximately half of the cells transfected with the Sgip1 853 isoform, we found an accumulation of the protein in the cytoplasm in the form of vesicles or inclusion bodies (Figure 7B').

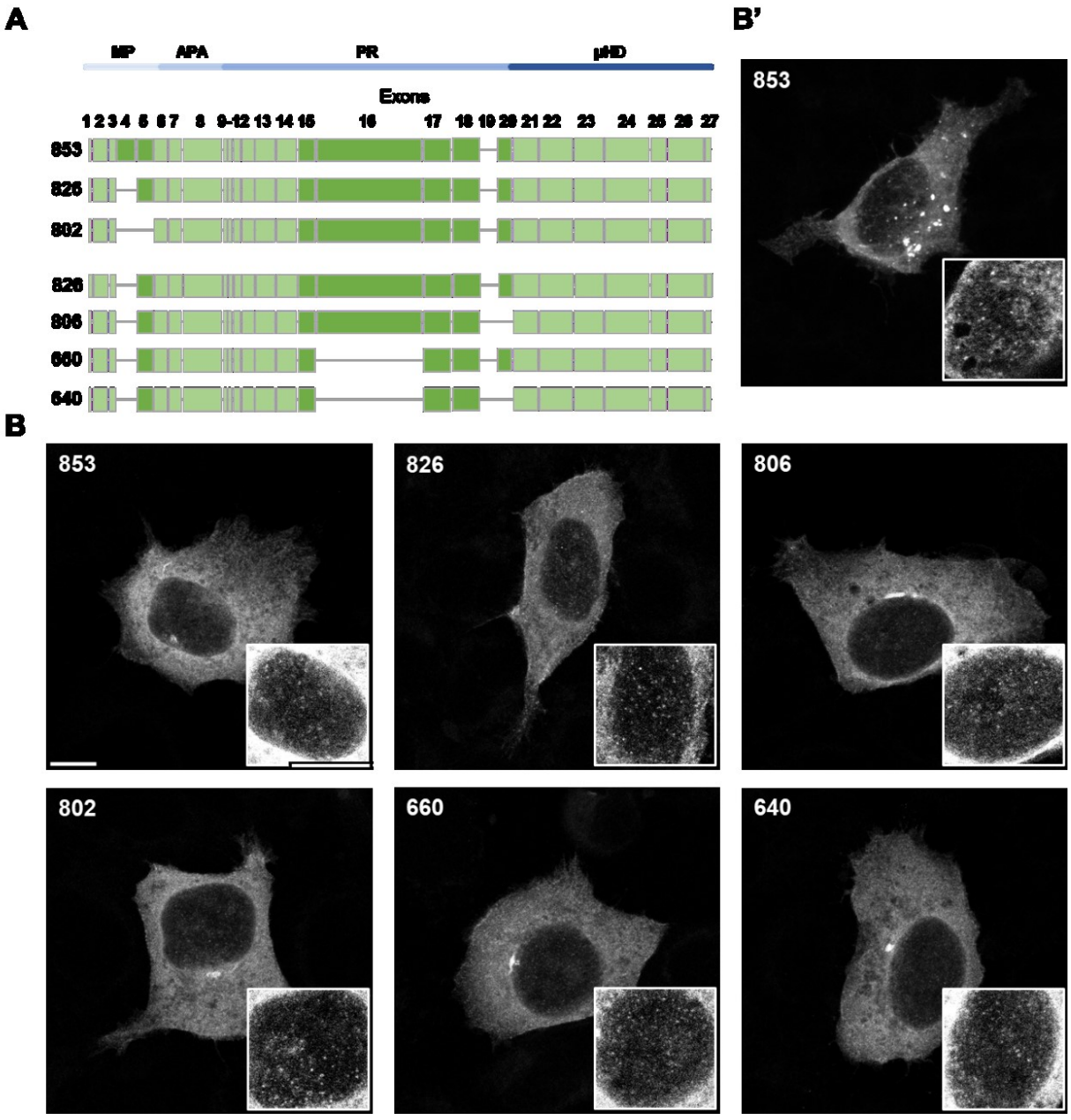


**Figure 7.** Expression of *Sgip1* splice variants in HEK293 cells. (A) The subset of the *Sgip1* splice variants chosen for testing, extracted from Figure 6. (B) The selected splice variants were analyzed under the confocal microscope. Some of the cells transfected with the Sgip1 853 variant showed accumulation of the protein in the cytoplasm (B'). Insets show membrane planes of the cells with enhanced brightness and contrast. Scale bar represents 10 µm. PFC - the prefrontal cortex, MP - membrane phospholipid-binding domain, APA - AP2 activator domain, PR - proline-rich region, µHD - µ homology domain.

### 4.3. Pharmacodynamic studies of the hexahydrocannabinol effect on CB1R

#### 4.3.1. Effects on G protein activation

We evaluated the G protein activation elicited by the hexahydrocannabinol (HHC) epimers (9S)-HHC and (9R)-HHC and compared their effects to those elicited by THC and WIN. (9S)-HHC had lower potency (logEC50 = -6.597) and efficacy than (9R)-HHC (logEC50 = -7.650) in the $G_{i1}$ activation assay (Figure 8A). The potency and efficacy of (9R)-HHC were similar to those of THC (logEC50 = -7.876). The potency of (9S)-HHC was similar to that of WIN (logEC50 = -6.818), but the efficacy of (9S)-HHC was much lower than that of WIN (Figure 8A).

In the $G_{oA}$ activation assay, the potency (logEC50 = -6.633) and efficacy of (9S)-HHC were lower than those of (9R)-HHC (logEC50 = -7.623) (Figure 8B). The potency and efficacy of (9R)-HHC were similar to those of THC (logEC50 = -8.069) and WIN (logEC50 = -7.223). Overall, the results indicate that the effect of (9R)-HHC epimer on the G protein activation is similar to that of THC, and (9S)-HHC has lower pharmacological activity.

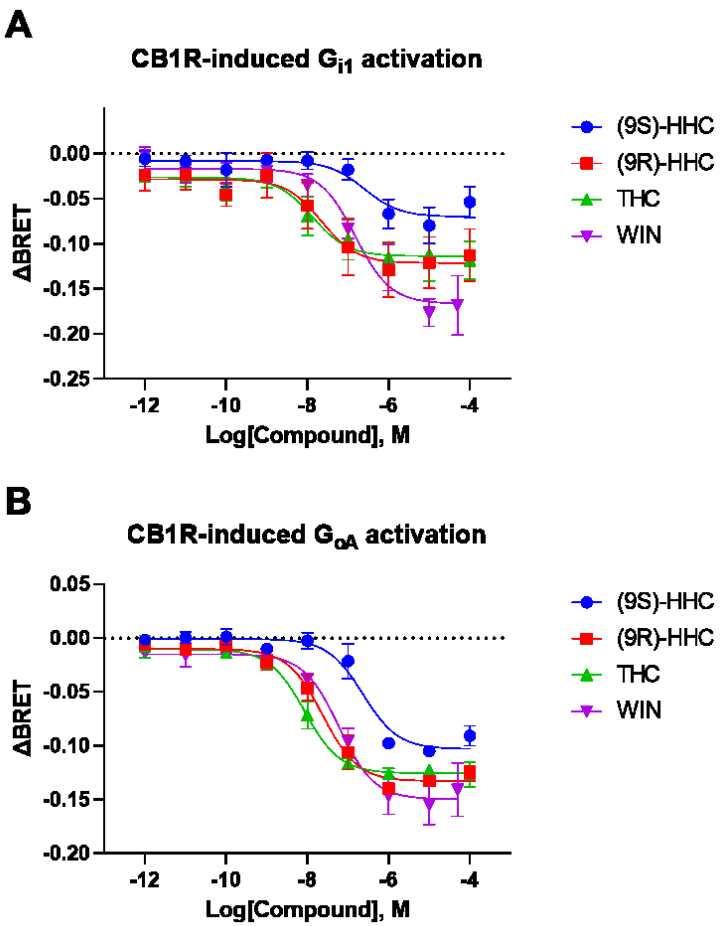


**Figure 8.** G protein activation induced by CB1R agonists. A) Dose-response relationship of $G_{i1}$ activation after CB1R stimulation. B) Dose-response relationship of $G_{oA}$ activation after CB1R stimulation. The data are presented as means ± SEM from three independent experiments.

### 4.3.2. Effects on GRK3 and β-arrestin signaling

We tested the GRK3-CB1R and β-arrestin 2-CB1R interactions elicited by the hexahydrocannabinol epimers (9S)-HHC and (9R)-HHC and compared their effects to the effects elicited by THC and WIN. (9S)-HHC, (9R)-HHC, and THC had a low ability to stimulate the interactions, as opposed to WIN, which had the highest potency and efficacy (Figure 9). (9S)-HHC had lower potency (logEC50 = -4.983) and efficacy than (9R)-HHC (logEC50 = -6.172) in the GRK3-CB1R interaction assay (Figure 9A). The potency of (9R)-HHC was similar to those of THC (logEC50

= -6.250) and WIN (logEC50 = -6.712), but (9R)-HHC had lower efficacy than WIN and higher potency than THC.

In the β-arrestin 2-CB1R interaction assay, (9S)-HHC and THC did not induce the interaction efficiently at the tested concentrations. The potency (logEC50 = -5.284) and efficacy of (9R)-HHC were lower than those of WIN (logEC50 = -6.344) (Figure 9B). Overall, the results indicate that (9R)-HHC epimer stimulates GRK3-CB1R and β-arrestin 2-CB1R interactions more effectively than THC, and the (9S)-HHC epimer, similar to THC, has a low ability to stimulate the interactions that result in desensitization of CB1R.

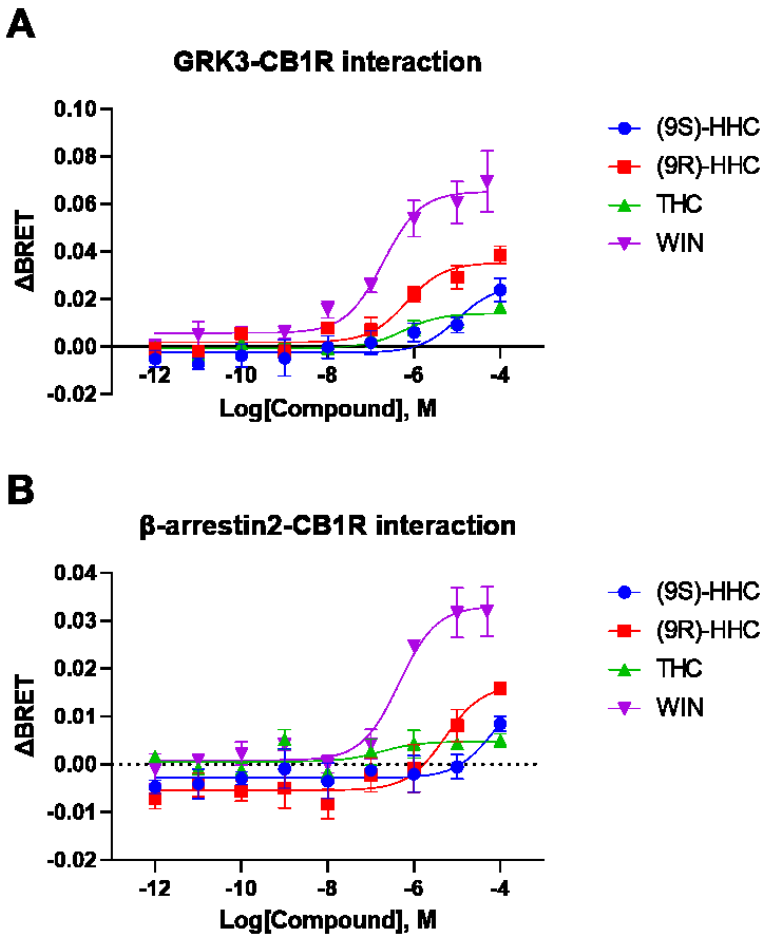


**Figure 9.** GRK3-CB1R and β-arrestin 2-CB1R interactions induced by CB1R agonists. A) Dose-response relationship of GRK3 recruitment to CB1R after CB1R stimulation. B) Dose-response relationship of β-arrestin 2 recruitment to CB1R after CB1R stimulation. The data are presented as means ± SEM from three independent experiments.

# 5. Discussion

## 5.1. The effect of Sgip1 on chronic pain processing

Our current and previous results suggest that Sgip1 is involved in the regulation of acute and chronic inflammatory pain. The effect of Sgip1 on pain perception could be explained by its interaction with CB1R, which is an essential component in the regulation of pain perception. The interaction of Sgip1 and CB1R affects the signaling of CB1R and, notably, inhibits the internalization of the receptor. Because of the inhibition of internalization, neuronal trafficking of CB1R may be altered, and CB1R may be retained at particular compartments, such as the axonal or synaptic plasma membrane. Indeed, several reports suggest that the mobility or trafficking of CB1R is restricted to particular neuronal compartments [26-28]. Sgip1 may stabilize such CB1R at axonal or synaptic compartments and, by means of that, optimize CB1R signaling and availability. Consequently, Sgip1 deletion would liberate CB1R, impair its polarized trafficking, and compromise its effects on neuronal circuits and, therefore, on behavior. In our previous study, we observed signs of altered CB1R activity in *Sgip1* knock-out mice, such as decreased anxiety-like behaviors and acute nociception, facilitated fear extinction to tone, and higher sensitivity to analgesics [12].

Long-term WIN incubations (for 16-17 h) result in a complete loss of CB1R surface staining in neuronal cultures [28, 29]. This observation might suggest the transient interaction of Sgip1 with CB1R, which ceases after prolonged stimulation of the receptor. CB1R may be persistently stimulated as a result of sensitization of the nervous system during chronic pain; therefore, the effect of Sgip1 on the receptor may be lost or altered. The increased sensitivity to chronic pain in the absence of Sgip1, which we observed in the current study, may result from this transient effect of Sgip1 on CB1R.

### 5.2. Identification and characterization of *Sgip1* splice variants in the brain

The patterns of *Sgip1* expression screened by immunoblotting and RT-PCR experiments predicted the presence of splice variants of *Sgip1* in the brain. The large number of exons that allow in-frame deletion in the *Sgip1* gene is likely responsible for this versatility of alternative splicing of *Sgip1*.

We detected 15 *Sgip1* splice variants resulting from the *Sgip1* gene alternative splicing in the mouse brain, four of which have been described previously. Due to the large number of the detected *Sgip1* splice variants, we indicate each *Sgip1* splice variant with its length.

Sgip1 domain architecture contains the membrane phospholipid-binding (MP) domain, AP2 activator (APA) domain, proline-rich region, and μ homology domain (μHD) [30, 31]. The alternative splicing pattern of *Sgip1* follows the domain structure of the Sgip1 protein. Spliced exons 4 and 5 lie within the MP domain, and spliced exons 9, 10, 15-20 lie within the proline-rich region (Figure 6).

Exons within the APA and μHD domains do not undergo alternative splicing (Figure 6). The APA domain was shown to interact with and activate the AP-2 complex [30]. The μHD interacts with endocytic adaptors and other proteins, such as EPS15 [24] and CB1R [9]. The absence of alternative splicing at the APA and μHD domain-coding exons underlines their functional importance because these domains preserve high homology between species and supports the notion that protein-protein interaction surfaces tend to be protected from exon removals [32].

We tested various Sgip1 splice isoforms to evaluate the effect of deletions of certain protein regions that are coded by the variable exons. The variable exons 4 and 5 are located within the MP domain (Figure 6). The MP domain binds negatively-charged membrane phospholipids and deforms membranes [33] by an undescribed mechanism. This mechanism may involve positively charged lysine, arginine, or histidine residues, which mediate interactions with membrane lipids in membrane-binding domains [34]. Our results suggest that the MP domain formed by exons 1-3 and a part of exon 6, containing eight lysine and four arginine residues,

may be sufficient to mediate Sgip1 binding to the plasma membrane. Therefore, exon variations in the MP domain do not limit Sgip1 interactions with plasma membrane lipids; however, these variations may affect the strength and specificity of the lipid binding or have a direct effect on protein interactions or dimerization.

The Sgip1 853 isoform showed an accumulation in the cytoplasm in the form of vesicles or inclusion bodies in about half of the transfected cells. The Sgip1 853 isoform differs from Sgip1 826 isoform only in the presence of exon 4; therefore, exon 4 may cause the unusual pattern of Sgip1 853 expression. Exon 4 encodes a stretch of three lysine residues that may cause an increase the protein aggregation and formation of the intracellular bodies. Besides the lysines, exon 4 encodes a cysteine residue that is followed by two aromatic residues. These amino acid motifs are conserved across species. Because exon 4 codes a sequence located within the MP domain, the MP domain may define the intracellular distribution of Sgip1.

We detected *Sgip1* splice variants with various exon combinations within the proline-rich region. Variations in exons 16 and 20 within the proline-rich region did not affect the protein's stability and localization. The proline-rich region of Sgip1 contains multiple potential phosphorylation sites [35, 36], SH3- and WW-domain binding domains [37]. Hyperphosphorylation of Sgip1 was found in the Huntington's disease mice [39]. Sgip1 was shown to be a substrate of MAP kinases [36], and its phosphorylation may therefore be physiologically significant. The mechanisms by which these sites mediate or regulate Sgip1's function or interaction with other endocytic proteins are unknown.

### 5.3. Pharmacodynamic studies of the hexahydrocannabinol effect on CB1R

Our results correspond to the previous findings demonstrating the higher affinity of (9R)-HHC to CB1R than that of (9S)-HHC [40]. (9R)-HHC was shown to be more potent in cannabinoid-related tests in mice than (9S)-HHC. (9R)-HHC significantly affected two behaviors of the cannabinoid tetrad test: hypolocomotion, reflecting reduced spontaneous movements, and analgesia, reflecting pain relief

[41]. However, the ability of (9R)-HHC to affect mouse behavior was lower than that of THC. These findings suggest that (9R)-HHC, but not (9S)-HHC, may have a CB1R-mediated psychotropic effect.

While we tested the pharmacological activities of the highly pure preparations of the HHC epimers, the HHC available in the market usually contains a mix of two epimers. Because these two epimers differ in potency and efficacy, the proportion of (9R)-HHC and (9S)-HHC defines the overall biological activity of such preparations.

The data on the safety of HHC is scarce. In one study, no toxic effects of HHC were observed up to HHC concentration of 50 uM, and HHC produced potential cytotoxic effects only when it exceeded the concentration of 10 mM [44]. These findings indicate that safe possible human consumption of THC is feasible without complications. However, contamination of HHC preparations with extraction residues or synthetic byproducts could pose unforeseen risks. Therefore, the HHC and other cannabinoid products on the market should be under close control of the authorities to ensure their quality and safety. In addition, more *in vitro* and *in vivo* studies are necessary to properly understand the effects of HHC on cell signaling and organism functions.

## 6. Conclusions

In this work, we studied the mechanisms influencing the signaling of cannabinoid receptor 1 (CB1R) on the molecular level and on the level of the organism. To study the role of SGIP1 in pain sensitivity, the alternative splicing of SGIP1, and the effect of minor cannabinoid hexahydrocannabinol (HHC) on CB1R, we employed various molecular biology and animal behavior approaches. These approaches included the behavioral testing of mechanical sensitivity, immunoblotting and PCR analysis, molecular cloning, light microscopy, and bioluminescence resonance energy transfer (BRET) assays.

First, we provide evidence that SGIP1 is an important player in inflammatory pain perception. Deletion of *Sgip1* resulted in the increase in chronic pain sensitivity in male but not in female mice during carrageenan-induced inflammation. After WIN or THC injections, *Sgip1* knock-out males preserved the increased nociception. The female mice had comparable pain thresholds after WIN application, but *Sgip1* knock-out female mice had higher pain thresholds after THC application than wild-type mice (Hypothesis 1, Aim 1).

Next, we cloned 15 *Sgip1* splice variants from the mouse brain. These splice variants result from alternative splicing of exons encoding the MP domain (exons 4 and 5) and proline-rich region (exons 9, 10, 15-20) of Sgip1 protein. Alterations within the MP domain or proline-rich region do not affect the stability of most Sgip1 splice isoforms and their subcellular localization (Hypothesis 2, Aim 2).

Further, we demonstrated that SGIP1 is a specific endocytic inhibitor of CB1R. SGIP1 inhibits CB1R internalization but do not affect internalization of other receptors, such as μ-opioid receptor and muscarinic acetylcholine M3 receptor.

Last, we evaluated the effects of HHC epimers (9S)-HHC and (9R)-HHC on CB1R signaling. We found that the potency and efficacy of (9R)-HHC to activate G proteins is higher than that of (9S)-HHC. However, the efficacy to cause GRK3 and β-arrestin 2 interactions with CB1R is similar for both (9R)-HHC and (9S)-HHC.

Moreover, the pharmacological profile of (9R)-HHC is closer to that of THC (Hypothesis 3, Aim 3).

Taken together, we demonstrate that SGIP1 is a specific CB1R-interacting protein, involved in CB1R-mediated chronic pain sensitivity. SGIP1 modulates pain processing pathways, resulting in decreased chronic pain sensitivity. The presence of multiple splice variants of SGIP1 suggests that expression of certain SGIP1 splice variants might be tailored to specific functions. The pharmacological activity of (9R)-HHC epimer, but not (9S)-HHC epimer, approximates that of THC. Due to the limited number of studies on HHC, its pharmacological potential should be assessed in future studies on its safety and biological action.

# 7. Summary

## 7.1. The effect of Sgip1 on chronic pain processing

We tested the chronic nociception in *Sgip1* knock-out and wild-type mice. We found that *Sgip1* deletion results in an increase in chronic nociception in male but not in female mice. The increased chronic nociception persisted in *Sgip1* knock-out male mice even after cannabinoid drug injections. Therefore, the effect of Sgip1 on CB1R results in decreased chronic pain sensitivity.

## 7.2. Identification and characterization of *Sgip1* splice variants in the brain

We addressed the discrepancies regarding the use of different *Sgip1* splice variants present in the literature. We cloned 15 *Sgip1* splice variants from the mouse brain and found that exons that undergo alternative splicing encode portions of the MP domain (exons 4 and 5) and proline-rich region (exons 9, 10, 15-20) of the Sgip1 protein. While most of *Sgip1* splice variants had similar properties, the intracellular localization of *Sgip1* variants containing exon 4 was distorted, and this variant accumulated in the intracellular vesicles or bodies.

We also tested the effect of SGIP1 on internalization of CB1R, μ-opioid receptor, and muscarinic acetylcholine M3 receptor. We found that SGIP1 is a specific endocytic inhibitor of CB1R, as SGIP1 does not affect internalization of μ-opioid receptor and muscarinic acetylcholine M3 receptor.

## 7.3. Pharmacological evaluation of hexahydrocannabinol epimers

We measured the CB1R-related G protein, GRK3, and β-arrestin 2 signaling of hexahydrocannabinol (HHC) epimers. We found that (9R)-HHC epimer has the pharmacological activity higher than that of (9S)-HHC in the G protein activation. However, (9R)-HHC and (9S)-HHC have comparable effects on GRK3- and β-arrestin 2-related signaling. Overall, the potency and efficacy of (9R)-HHC is similar to that of THC.

## 8. Literature references


1. Zou, S.L. and U. Kumar, *Cannabinoid Receptors and the Endocannabinoid System: Signaling and Function in the Central Nervous System.* International Journal of Molecular Sciences, 2018. **19**(3): p. 23.
2. Herkenham, M., et al., *Characterization and Localization of Cannabinoid Receptors in Rat-Brain - a Quantitative Invitro Autoradiographic Study.* Journal of Neuroscience, 1991. **11**(2): p. 563-583.
3. Herkenham, M., et al., *Cannabinoid Receptor Localization in Brain.* Proceedings of the National Academy of Sciences of the United States of America, 1990. **87**(5): p. 1932-1936.
4. Howlett, A.C., et al., *The Cannabinoid Receptor - Biochemical, Anatomical and Behavioral Characterization.* Trends in Neurosciences, 1990. **13**(10): p. 420-423.
5. Mackie, K., *Distribution of cannabinoid receptors in the central and peripheral nervous system.* Handbook of Experimental Pharmacology, 2005(168): p. 299-325.
6. Bridges, D., et al., *Localisation of cannabinoid receptor 1 in rat dorsal root ganglion using in situ hybridisation and immunohistochemistry.* Neuroscience, 2003. **119**(3): p. 803-812.
7. Chaperon, F. and M.H. Thiebot, *Behavioral effects of cannabinoid agents in animals.* Critical Reviews in Neurobiology, 1999. **13**(3): p. 243-281.
8. Viveros, M.P., E.M. Marco, and S.E. File, *Endocannabinoid system and stress and anxiety responses.* Pharmacology Biochemistry and Behavior, 2005. **81**(2): p. 331-342.
9. Hajkova, A., et al., *SGIP1 alters internalization and modulates signaling of activated cannabinoid receptor 1 in a biased manner.* Neuropharmacology, 2016. **107**: p. 201-214.
10. Fletcher-Jones, A., et al., *SGIP1 binding to the α-helical H9 domain of cannabinoid receptor 1 promotes axonal surface expression.* bioRxiv, 2023: p. 2023.07.18.549510.
11. Gazdarica, M., et al., *SGIP1 modulates kinetics and interactions of the cannabinoid receptor 1 and G protein-coupled receptor kinase 3 signalosome.* Journal of Neurochemistry, 2021.
12. Dvorakova, M., et al., *SGIP1 is involved in regulation of emotionality, mood, and nociception and modulates in vivo*

*signalling of cannabinoid CB1 receptors.* British Journal of Pharmacology, 2021. **178**(7): p. 1588-1604.
13. Francis, D.L. and C. Schneider, *Jumping after Naloxone Precipitated Withdrawal of Chronic Morphine in Rat.* British Journal of Pharmacology, 1971. **41**(2): p. P424-+.
14. Lee, S.-E., et al., *SGIP1α functions as a selective endocytic adaptor for the internalization of synaptotagmin 1 at synapses.* Molecular Brain, 2019. **12**(1): p. 41.
15. Li, H.D., W.X. Liu, and M. Michalak, *Enhanced Clathrin-Dependent Endocytosis in the Absence of Calnexin.* Plos One, 2011. **6**(7): p. 11.
16. Lee, S.E., et al., *SGIP1alpha, but Not SGIP1, is an Ortholog of FCHo Proteins and Functions as an Endocytic Regulator.* Frontiers in Cell and Developmental Biology, 2021. **9**: p. 801420.
17. Gaoni, Y. and R. Mechoulam, *Hashish .7. Isomerization of Cannabidiol to Tetrahydrocannabinols.* Tetrahedron, 1966. **22**(4): p. 1481-+.
18. Casati, S., et al., *Hexahydrocannabinol on the Light Cannabis Market: The Latest "New" Entry.* Cannabis and Cannabinoid Research, 2022.
19. Ujvary, I., *Hexahydrocannabinol and closely related semi-synthetic cannabinoids: A comprehensive review.* Drug Testing and Analysis, 2023.
20. Ujvary, I., et al., *Hexahydrocannabinol (HHC) and related substances*, in *TECHNICAL REPORT*. 2023. p. 1-106.
21. Tanaka, R. and R. Kikura-Hanajiri, *Identification of hexahydrocannabinol (HHC), dihydro-iso-tetrahydrocannabinol (dihydro-iso-THC) and hexahydrocannabiphorol (HHCP) in electronic cigarette cartridge products.* Forensic Toxicology, 2023.
22. Wobbrock, J.O., et al., *The Aligned Rank Transform for Nonparametric Factorial Analyses Using Only ANOVA Procedures.* 29th Annual Chi Conference on Human Factors in Computing Systems, 2011: p. 143-146.
23. Schindelin, J., et al., *Fiji: an open-source platform for biological-image analysis.* Nature Methods, 2012. **9**(7): p. 676-682.
24. Uezu, A., et al., *SGIP1 alpha is an endocytic protein that directly interacts with phospholipids and Eps15.* Journal of Biological Chemistry, 2007. **282**(36).

25. Wilhelm, B.G., et al., *Composition of isolated synaptic boutons reveals the amounts of vesicle trafficking proteins.* Science, 2014. **344**(6187): p. 1023-1028.
26. Mikasova, L., et al., *Altered surface trafficking of presynaptic cannabinoid type 1 receptor in and out synaptic terminals parallels receptor desensitization.* Proceedings of the National Academy of Sciences of the United States of America, 2008. **105**(47): p. 18596-18601.
27. Simon, A.C., et al., *Activation-dependent plasticity of polarized GPCR distribution on the neuronal surface.* Journal of Molecular Cell Biology, 2013. **5**(4): p. 250-265.
28. McDonald, N.A., et al., *An essential role for constitutive endocytosis, but not activity, in the axonal targeting of the CB1 cannabinoid receptor.* Molecular Pharmacology, 2007. **71**(4): p. 976-984.
29. Coutts, A.A., et al., *Agonist-induced internalization and trafficking of cannabinoid CB1 receptors in hippocampal neurons.* Journal of Neuroscience, 2001. **21**(7): p. 2425-2433.
30. Hollopeter, G., et al., *The Membrane-Associated Proteins FCHo and SGIP Are Allosteric Activators of the AP2 Clathrin Adaptor Complex.* Elife, 2014. **3**: p. 65.
31. Reider, A., et al., *Syp1 is a conserved endocytic adaptor that contains domains involved in cargo selection and membrane tubulation.* Embo Journal, 2009. **28**(20): p. 3103-3116.
32. Colantoni, A., et al., *Alternative splicing tends to avoid partial removals of protein-protein interaction sites.* Bmc Genomics, 2013. **14**.
33. Trevaskis, J., et al., *Src homology 3-domain growth factor receptor-bound 2-like (endophilin) interacting protein 1, a novel neuronal protein that regulates energy balance.* Endocrinology, 2005. **146**(9): p. 3757-3764.
34. Lemmon, M.A., *Membrane recognition by phospholipid-binding domains.* Nature Reviews Molecular Cell Biology, 2008. **9**(2): p. 99-111.
35. Craft, G.E., et al., *The in vivo phosphorylation sites in multiple isoforms of amphiphysin I from rat brain nerve terminals.* Molecular & Cellular Proteomics, 2008. **7**(6): p. 1146-1161.

36. Edbauer, D., et al., *Identification and Characterization of Neuronal Mitogen-activated Protein Kinase Substrates Using a Specific Phosphomotif Antibody.* Molecular & Cellular Proteomics, 2009. **8**(4): p. 681-695.
37. Zarrinpar, A., R.P. Bhattacharyya, and W.A. Lim, *The Structure and Function of Proline Recognition Domains.* Science's STKE, 2003. **2003**(179): p. re8-re8.
38. Munton, R.P., et al., *Qualitative and quantitative analyses of protein phosphorylation in naive and stimulated mouse synaptosomal preparations.* Molecular & Cellular Proteomics, 2007. **6**(2): p. 283-293.
39. Mees, I., et al., *Phosphoproteomic dysregulation in Huntington's disease mice is rescued by environmental enrichment.* Brain Communications, 2022. **4**(6).
40. Reggio, P.H., K.V. Greer, and S.M. Cox, *The Importance of the Orientation of the C9 Substituent to Cannabinoid Activity.* Journal of Medicinal Chemistry, 1989. **32**(7): p. 1630-1635.
41. Russo, F., et al., *Synthesis and pharmacological activity of the epimers of hexahydrocannabinol (HHC).* Scientific Reports, 2023. **13**(1): p. 11061.
42. Archer, R.A., et al., *STRUCTURAL STUDIES OF CANNABINOIDS - A THEORETICAL AND PROTON MAGNETIC RESONANCE ANALYSIS.* Journal of the American Chemical Society, 1970. **92**(17): p. 5200-&.
43. Turner, C.E., et al., *CONSTITUENTS OF CANNABIS-SATIVA L .4. STABILITY OF CANNABINOIDS IN STORED PLANT MATERIAL.* Journal of Pharmaceutical Sciences, 1973. **62**(10): p. 1601-1605.
44. Collins, A.C., et al., *Nonclinical In Vitro Safety Assesment Summary of Hemp Derived (R/S)-Hexahydrocannabinol ((R/S)-HHC).* [Preprint] Research Square, 2022.

## 9. List of the author's publications

**Publications related to the thesis:**

1. **Durydivka O.**, Gazdarica M., Vecerkova K., Radenkovic S., Blahos J. Multiple Sgip1 Splice Variants Inhibit Cannabinoid Receptor 1 Internalization. Gene. **2023** 147851 doi: 10.1016/j.gene.2023.147851 PMID: 37783296. (IF= 3.913)
2. Gazdarica M., Noda J., **Durydivka O.**, Novosadova V., Mackie K., Pin J.-P., Prezeau L., Blahos J. SGIP1 modulates kinetics and interactions of the cannabinoid receptor 1 and G protein-coupled receptor kinase 3 signalosome. Journal of Neurochemistry. **2022** 160:625-642 doi: 10.1111/jnc.15569 PMID: 34970999. (IF= 5.546)
3. **Durydivka O.**, Mackie K., Blahos J. SGIP1 in axons prevents internalization of desensitized CB1R and modifies its function. Frontiers in Neuroscience. **2023** 17:1-11 doi: 10.3389/fnins.2023.1213094 PMID: 37547151. (IF= 5.152)

## Overview of the author's presentations

- *SGIP1 as a modulator of cannabinoid receptor 1* (presentation). 16th IMG PhD conference, Institute of Molecular Genetics of the Czech Academy of Sciences, 2023.
- *Altered acute and chronic nociception in SGIP1 knock-out mice* (poster). Cannabinoid Function in the CNS, Gordon Research Seminar and Conference, Castelldefels, Spain, 2023.
- *Regulation of cannabinoid receptor 1 signaling by SGIP1* (presentation). Regular Wednesday IMG seminar, Institute of Molecular Genetics of the Czech Academy of Sciences, 2022.
- *Altered nociception in SGIP1 knock-out mice* (poster). Scientific Conference at the Second Faculty of Medicine of the Charles University, 2022.
- *SGIP1 modulates acute and chronic nociception in a sex-specific fashion* (poster). 32nd Annual International Cannabinoid Research Society Symposium on the Cannabinoids, National University of Ireland, Galway, Ireland, 2022.
- *SGIP1 modulates cannabinoid receptor 1 desensitization and internalization* (poster). 21st Great Lakes GPCR retreat, University of Toronto, Niagara-on-the-Lake, Canada, 2022.